Digest Journal of Nanomaterials and Biostructures Vol. 12, No. 2, April - June 2017, p. 605 - 613

FUNCTIONALIZED SELF-ASSEMBLING PEPTIDE NANOFIBER SCAFFOLDS FOR CULTURING MC3T3-E1 CELLS

X. CHEN, A. ZHOU, W. ZHAO, S. CHEN, B. HE, D. JIANG*
Department of Orthopedics, The First Affiliated Hospital of Chongqing Medical University, Chongqing, China, 400016;

It was important to recapitulate the topographical and biochemical features of extracellular matrix for functional biomimetic scaffolds. In this study, functionalized peptide nanofiber scaffold was developed to simulate the critical features of native bone tissue. Functional motif RGD was conjugated to RADA16 to form RADA16-RGD which could self-assemble into interwoven peptide nanofiber structures. Results demonstrated that combination of RADA16-RGD and RADA16 nanofibers was associated with improved adhesion, spreading, proliferation and osteogenic differentiation of MC3T3-E1 cells than pure RADA16 scaffold. This peptide-decorated scaffolds hold some potential in bone tissue engineering.

(Received April 15, 2017; Accepted June 14, 2017)

Keywords: Molecular self-assembly, RGD, RADA16 self-assembling peptide, Nanofiber scaffolds, Bone tissue engineering.

1. Introduction

The occurrence of bone defect associated with tumors, osteoporosis, and osteoarthritis has become increasing and required growing expenditure for health care every year [1]. Invasive surgeries using metallic/polymeric implants or autografts were the predominant approaches for bone defects [2]. Autologous grafts with good osteogenic, osteoinductive and osteoconductive ability were known as the gold standard to repair bone defects [3], but they were limited by pain, donor-site morbidity, the mismatch between harvested bone grafts and defect sites, as well as insufficient quantity [4, 5]. Synthetic material scaffolds involving metal materials, polymers, bioceramics, bioglass, and composite materials showed some shortcomings such as relatively low osteoinductivity and osteoconductivity, the difficulty in degradation or even non-degradation [6-8].

More recently, ionic self-complementary peptides self-assembly into nanofiber scaffolds have emerged as an important alternative for culturing bone cells and improving bone regeneration. Previous studies have demonstrated the potential of peptide nanofiber scaffolds in repairing damaged tissues or organs including cartilage [9, 10], bone [11-13], nerve [14, 15], heart [16, 17], as well as wound healing [18, 19]. It was gradually recognized that among various parameters influencing cell–material interactions, not only topographical but also biochemical cues should be considered in the design of scaffold materials in order to mimic the chemical and physical features of microenvironments in native tissues [20]. The functionalization of nanofibers with bioactive factors became increasingly important to construct bone biomimetic scaffolds presenting multiple cues for the regulation of cell fates. Many biomolecules were found to be tethered to the native ECM and mediate cell function, which inspired the functionalization modification of nanofiber scaffolds using functional proteins. Many functional motifs (e.g. RGD [21], IKVAV [22] and YIGSR [23]) were developed to tailor biomaterial scaffolds. The tripeptide sequence RGD could bind to α5β1 integrin receptor and induce cell differentiation and migration [24], and assist in the maintenance of chondrocyte number and phenotype, as well as the increase in ECM contents [25]. Peptide RADA16 and peptide RADA16-IKVAV were combined to form IKVAVmx hydrogel scaffolds which substantially improved cellular proliferation, differentiation and migration of neural stem cells [26].

*Corresponding author: jdm571026@vip.163.com

To the best of our knowledge, this was the first report that the presented biomimetic RADA16-RGD nanofiber and RADA16 nanofiber were combined to promote osteogenesis of bone cells. To evaluate the cytocompatibility and osteogenic activity of these materials, the adhesion, growth, and differentiation of MC3T3-E1 cells cultured on the peptide-decorated nanofibers were deeply investigated *in vitro*.

2. Experimental

2.1. Peptides synthesis and purification

Peptide RADA16-I sequence was Ac-(Arg-Ala-Asp- Ala-Arg-Ala-Asp-Ala)$_2$-CONH$_2$, and RADA16-RGD sequence was Ac-(Arg-Ala-Asp-Ala-Arg-Ala-Asp-Ala)$_2$-Gly-Gly-Arg-Gly-Asp-Ser-CONH$_2$. These peptides were commercially custom-synthesized by solid-phase peptide synthesis (Shanghai Biotech Bioscience and Technology Co, Ltd, Shanghai, China). The peptides were acetylated and amidated on the N-terminus and C-terminus, respectively. Purified by HPLC and characterized by mass spectroscopy. The purity of the RADA16-I and RADA16-RGD were 97.45% and 95.00%, respectively.

2.2. Circular dichroism spectroscopy

The peptide samples consisted of 1.0 mg/ml peptide aqueous stock dissolved and were adjusted to 25 μM using 20 mM Nacl. Measurements were carried out on circular dichroism (CD) spectrometer (JASCO Corporation, J-810, Japan) at 25℃. The data were collected using a CD cuvette with a 5 mm path-length and measured from 190 to 290 nm.

2.3. Cell culture

The pre-osteoblastic MC3T3-E1 cells were obtained from American Type Culture Collection (ATCC), USA. 10mg/ml (w/v) peptide stock solution was prepared by dissolving lyophilized peptide powder in sterile water. There were three groups for this study. Control group: no hydrogel scaffold for cell culture. RADA16-I group: combining RADA16-I (10mg/ml) with PBS (pH 7.4) in the volume ratio of 1:1 to obtain 5mg/ml RADA16-I hydrogel. RGDmx group: mixing RADA16-RGD (10mg/ml), RADA16-I (10mg/ml) with PBS (pH 7.4) in the volume ratio of 4:1:5 to obtain RGDmx hydrogel. 100 ul peptide hydrogels were added in each well for at least 30 minutes. Empty wells filled with 100 ul PBS were used as the control group. Cells prepared for 2D cell culture were grown in DMEM/F-12 culture medium (HyClone) supplemented with 10% fetal bovine serum (Gibco) or osteogenesis induction medium. We observed cells through an inverted microscope (Olympus Corporation, Tokyo, Japan).

2.4. Cell morphology observation

Cells cultured on the hydrogel scaffolds were washed with phosphate buffer saline (PBS, 37℃) and fixed in 4% paraformaldehyde/PBS at 4℃ for 30 min. After three washings with PBS, the cultures were permeabilized using 0.1% Triton X-100 (Sigma, USA) for 10 min. Finally, the cultures were incubated with 5ug/ml rhodamine phalloidin (Sigma, USA) at room temperature for 40 min. The treated cultures were washed with PBS three more times in order to remove residual dye. The cultured cell scaffolds were then observed by fluorescence microscope (Nikon, A1R, Japan).

2.5. Cell proliferation

CCK-8 assay was applied to investigate cell viability. CCK-8 kit (Beyotime Biotechnology, China) was added into the culture medium of wells in the ratio of 1:10, and then the 24-multiwell plate was incubated at 37° C for 1 hour. The absorbance was measured using a VersaMax microplate reader (Thermo Electron Corporation, USA) at an absorption wavelength of 450 nm. The data was expressed as arbitrary absorbance units.

2.6. Alkaline phosphatase (ALP) activity

For quantitative ALP assay, the supernatants were collected for ALP assay using Alkaline Phosphatase Determination Kits (Beyotime Biotechnology, China) following manufacturer's protocol. Protein concentrations of the cell lysates were determined by monitoring the absorbance of the solution at a wavelength of 405 nm.

2.7. Alizarin Red S staining

Alizarin Red S staining was used to detect matrix mineralization of cells. These were rinsed with phosphate-buffered saline three times and fixed with 4% paraformaldehyde after 21 days of coculture. Next, 1 mL of 0.5% Alizarin Red S (Cyagen, China) solution was added and incubated for 10 minutes at room temperature. The staining result was observed using a light microscope (Olympus, Tokyo, Japan).

2.8. Western Blotting

Cells were harvested after 3 weeks. Protein samples (25 μg) were separated by sodium dodecyl sulfate-polyacrylamide gel electrophoresis (10%) and transferred to poly vinylidene fluoride membranes. After blocking with skimmed milk (5%) in TBS containing 0.05% Tween-20 (TBST) for 1 hour, the membranes were incubated overnight at 4° C with primary antibodies: anti-β-actin (1:3,000; TDY051, TDY, beijing, China), anti-Col-I (1:1,000; ab34710, Abcam, USA) and anti-osteopontin (OPN) (1:1,000; ab8448, Abcam, USA), followed by washing thrice with TBST. Afterward, the membranes were incubated with horseradish peroxidase-conjugated secondary antibodies (1:3,000; Boster, China) for 1 hour at RT. After washing thrice with TBST, the horseradish peroxidase reaction product was detected by ECL Western Blotting kit.

2.9. Statistics and data analysis

All datas were presented as the mean±standard deviation (SD). Differences between groups were determined using an unpaired Student's t-test. The differences were considered significant if $p < 0.05$.

3. Results and discussion

Material scaffolds were regarded as one key element of bone tissue engineering to provide physical support and good bioactivity for cellular function [27-30]. A novel biomaterial scaffold, ionic self-complementary peptides were found to self-assemble into nanofiber scaffolds highly mimicing the microstructure of natural ECM [31]. These self-assembling peptides were featured by alternating hydrophobic sides (e.g. alanine, valine, leucine, isoleucine, and phenylalanine), and hydrophilic sides including positively charged amino acid (e.g. lysine, arginine, histidine) and negatively charged amino acids (e.g. aspartic acids and glutamic acids) [31, 32]. The hydrophilic surface of the molecules with charged amino acid residues was critical to induce the peptide self-assembly and thus complementary ionic sides were divided into several moduli, such as modulus I, II, III, IV and mixed moduli: modulus I, -+ - + - + - +; modulus II, - - + + - - + + ; modulus III,---+++; and modulus IV,----++++ [31-37]. The design of charge orientation in reverse orientations can produce entirely different molecules with distinct molecular behaviors [31, 32, 38]. Indeed, many ionic self-complementary peptides including RAD16-I, RAD16-II, EAK16-I, EAK16-II, and d-EAK16 were developed for tissue engineering [19, 20, 33, 37].

It was known that controlled delivery of signal molecules was important to mediate cell-cell and cell-matrice interactions regulating cell function and tissue regeneration [39-44]. Previous studies demonstrated that functional proteins were allowed to slow release within RADA16-I peptide nanofiber scaffolds, and they mainly included basic-fibroblast growth factor (βFGF), vascular endothelial growth factor (VEGF) and brain-derived neurotrophic factor (BDNF). The secondary and tertiary structure analyses and biological assays confirmed the original protein conformation and functionality of released functional proteins were maintained [44, 45]. For instance, the released bone morphogenetic protein 2 (BMP2) from peptide nanofiber scaffolds promoted homogeneous ectopic bone formation in the back subcutis of rats [46]. Moreover, peptide epitopes (i.e. functional motifs) were extensively developed to coat biomaterials scaffolds in order to increase bioactivity through simulating the cell interaction of native ECM [32, 47]. Many studies reported that RGD [21], IKVAV[22], YIGSR [23] and PHSRN [48] used to modify self-assembling peptide hold important promise to modulate cellular function. Functional motifs (e.g. ALK, DGR and PRG)-modified RAD16 peptide hydrogels were added to pure RADA16 hydrogel and found to significantly improve attachment, proliferation, migration and osteogenic differentiation of MC3T3-E1 cells [49] In addition, RGD and OPD-coated nanofiber hydrogels showed some potential in reinforcing osteogenic differentiation [50, 51].

Our study focused on combining RADA16 hydrogel with RADA16-RGD hydrogel to produce RGDmx hydrogel and exploring its potential for spreading, proliferation and osteogenic differentiation of MC3T3-E1. The CD spectrum of peptide RADA16-RGD showed a maximum ellipticity at 194.5 nm and a minimum ellipticity at 198.5 nm at 25℃ (Fig. 1). When raising the concentration to 50 uM, The CD spectrum of peptide RADA16-RGD showed a maximum ellipticity at 193.5 nm and a minimum ellipticity at 198 nm at 25℃ [20]. These indicated that peptide RADA16-RGD could produce stable β-sheet secondary structure despite low concentration. Our previous study confirmed that peptide RADA16-RGD and RADA16 could form interwoven nanofibers networks following the stimulus of ion strength [20], and this study would mixing RADA16-RGD nanofibers with RADA16 nanofibers in the volume ratio of 4:1 to culturing MC3T3-E1 cells.

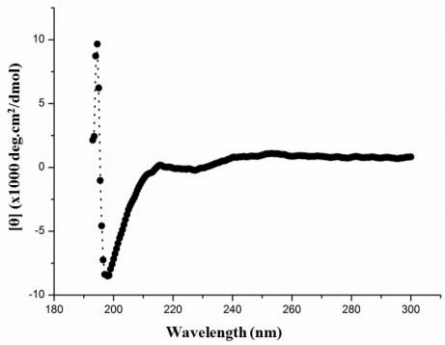

Fig. 1 Circular dichroism spectra of the chiral peptides. 25 μ M RADA16-RGD hydrogel in 20 mM NaCl at 25°C

3.1. Cell morphology observation

The morphology of MC3T3-E1 cells cultured on RADA16 and RGDAmix peptide scaffolds were determined by using a fluorescence microscope. As showed in Fig. 2, cells seemed to be adhering on both scaffolds with numerous pyknic cellular processes on 3 days. MC3T3-E1 cells spread on RADA16 and RGDAmix peptide scaffolds and the cells on RGDAmix scaffold appeared showing longer and larger cellular processes compared to RADA16 peptide scaffolds and especially to control group on 14 days. The cells cultured on RGDAmix scaffold were more elongated and exhibited numerous cellular processes, in contrast to the more slim morphology of MC3T3-E1 cells on RADA16 scaffold. These results indicated that RGDAmix scaffold showed better cell adhesion and spreading than RADA16 peptide scaffolds because of the function of RGD incorporated into peptide hydrogels.

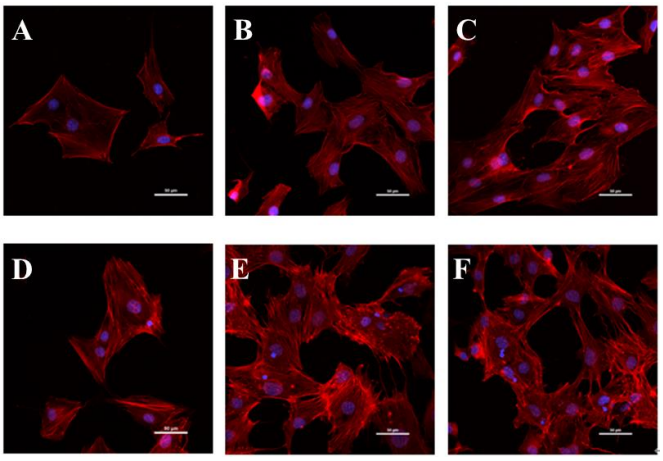

Fig. 2 Fluorescence observation of MC3T3-E1 cells on day 3 (A-C) and 7 (D-F), and cells were cultured in control group (A, D), RADA16 hydrogel (B, E), RGDmx hydrogel (C, F).

3.2. Cell proliferation

Successful engineered scaffolds were not only supportive of cell adhesion but also to improve cell proliferation. Fig. 3 showed that all test groups exhibited good time-dependent cell growth. However, lower optical density value was observed in all experimental groups compared with control group during incubation, indicating somewhat negative influence on cell growth of nanofibers, regardless of orientation and surface chemistries. The possible explanation was that the scaffold in pursuit of osteogenic differentiation might inhibit cell proliferation to some extent [52]. In addition, this could be further confirmed that under osteoinductive condition, MC3T3-E1 cells showed lower proliferation than those under non-osteoinductive condition. However, clearly on 3, 5, 7 days of incubation under non-osteoinductive condition or osteoinductive condition, Fig. 3 demonstrated that cells in RGDAmix peptide scaffolds showed significantly higher proliferation compared to RADA16 peptide scaffold, suggesting that functional modification with RGD peptides could endow the nanofibers with more desirable proliferation.

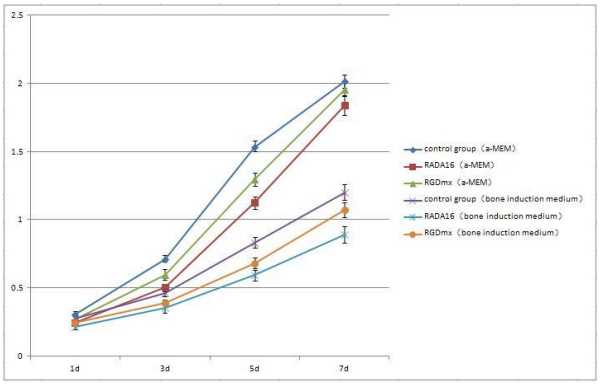

Fig. 3. CCK-8 method for cell proliferation: cells cultured within a-MEM or bone induction medium on day 1, 3, 5, 7

3.3. Osteogenic differentiation under osteoinductive conditions

To evaluate the osteogenic bioactivity of peptide-decorated nanofibers, the extent of osteogenesis in MC3T3-E1 cells on functionalized nanofibers was assessed under osteoinductive condition. Among the major osteogenic hallmarks, the upregulation of ALP activity was considered a key event occurring during the early time points of osteogenesis [1]. As shown in Fig. 4, compared to control group, all test groups demonstrated an enhancement in ALP activity. On 1 day, there was no significant difference between RGDAmix peptide scaffold, RADA16 peptide scaffolds and control group. From day 3 to 7, all groups showed an increased trend of ALP activity. Two hydrogel scaffold groups revealed significantly higher ALP activity compared to control group. And ALP activity in RGDAmix peptide scaffold was highest among three groups and had with a peak at 7 days due to the immobilization of RGD peptides on the nanofiber, suggesting the positive influence of RGD-functional nanofibers on the osteogenic differentiation of MC3T3-E1 cells. After 7 days, ALP activity in all groups maintained relatively high level. This finding revealed that the presence of RGD peptide on the nanofiber was capable of triggering an upregulation of ALP, correlated with the first checkpoint for osteogenic differentiation.

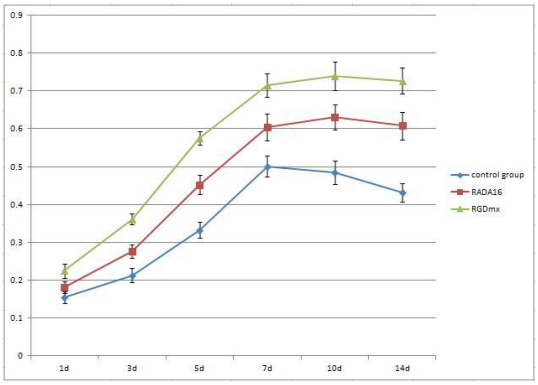

Fig. 4. ALP activity of MC3T3-E1 cells cultured on control group, RADA16 hydrogel, RGDmx hydrogel on day 1, 3, 5, 7, 10, 14

The production of calcium deposit at late stage of differentiation was another critical indicator for osteogenic efficiency of MC3T3-E1 cells [53]. As the osteogenic culture of MC3T3-E1 cells on functionalized nanofibers progressed to 21 days, cells aggregated together and formed bone-like structures that were stained for Alizarin Red S (Fig. 5). Similar to the trend observed with ALP activity, more calcium nodules and denser red staining were detected on RGDAmix peptide in comparison with RADA16 peptide scaffolds and control group, suggesting the osteogenic advantages of peptide nanofibers. Particularly, due to the conjugation of RGD peptides on nanofibers, a significant increment in the amount of mineralized matrix was observed in RGDAmix peptide. MC3T3-E1 cells on RGD peptide-conjugated nanofibers showed the highest production of calcium nodules among all groups by day 21 ($P < 0.01$). This result suggested that biochemical cues arising from RGD peptides may play a greater role in the osteogenic differentiation of MC3T3-E1 cells.

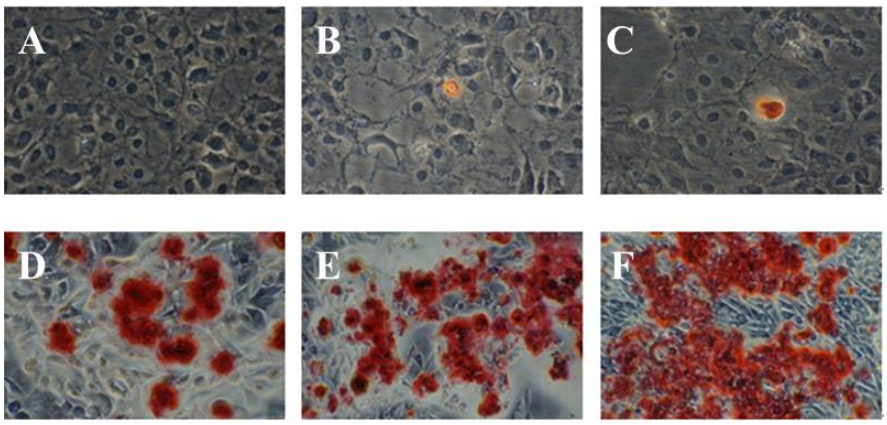

Fig. 5. Alizarin Red S staining of MC3T3-E1 cells cultured on control group (A, D), RADA16 hydrogel (B, E), RGDmx hydrogel (C, F)on day 7 (A-C), 21 (D-F)

To better understand the cellular interactions with functionalized nanofibers at transcript level, the expressions of osteo-specific genes were analyzed on day 21 (Fig. 6). The fold change of target genes was normalized to control MC3T3-E1 cells. Of all the osteo-related genes, collagen-I (Col-I) and OPN were regarded as the important specific marker for the mature osteoblast and mineralization during the course of osteogenesis. It accumulated in the calcified bone due to its

high affinity to hydroxyapatite crystals. As shown in Fig. 6, Col-I gene was unregulated in RGDAmix peptide group in comparison with RADA16 peptide group and control group. When cells were cultured with RGD peptide-decorated nanofibers, even higher expression of col-I was detected compared to peptide-unmodified group. Clearly, the modification of RGD peptides on nanofibers could further elevated the col-I expression, which was also confirmed along with another osteo-specific protein OPN by western blot analysis (Fig. 6).

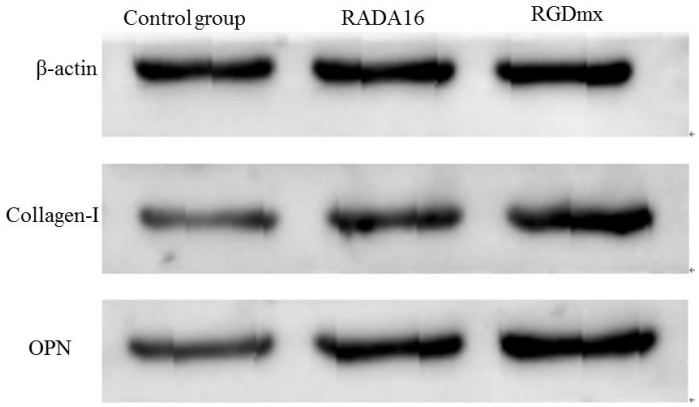

Fig. 6. Western blotting of β-actin, collagen-I, and OPN

Moreover, self-assembly peptide scaffolds were known as one kind of hydrogel structures suitable to serve as filling materials for bone defects. But the mechanical force of peptide hydrogels was relatively weak and they could not provide sufficient mechanical support to very large bone defects or load-bearing bone defects. Therefore, combining peptide scaffolds with other materials with good mechanical strength was an important approach to broaden the application of peptide hydrogel with good bioactivity [9]. Many studies reported peptide-based composite scaffolds for bone healing. For instance, peptide amphiphiles (PAs) hydrogels were utilized to fill the porosity of Ti-6Al-4V foam to fabricate hybrid bone implant materials (PA-Ti hybrid material) which significantly promote bone regeneration around and inside the implant, as well as vascularization when treating the diaphysis defects of the hind femurs of SD rats, and revealed some promise in improving fixation, osteointegration and long term stability of implants [54]. A load-bearing polymer matrix was combined with peptide scaffolds to synthesize composite material which had good mechanical strength and osteoinductivity for bone healing [55].

4. Conclusions

In this study, RGD-decorated peptide nanofibers with highly network structures that simulated the crucial characteristics of native bone tissue were developed via peptide self-assembly and regulate osteoblast differentiation of MC3T3-E1 cells. Our results demonstrated that the functional modification of RGD peptides on nanofibers could improve MC3T3-E1 cells adhesion, spreading and proliferation. RGD-conjugated peptide nanofibers could further enhance the osteogenic differentiation of MC3T3-E1 cells. Other experiments are in progress to investigate whether the combination of RGD-conjugated peptide nanofibers and growth factors could realize

the synergistic effect on bone formation in vivo as well as in vitro. We believe the presented study provided an instructive insight in designing biomimetic scaffolds targeted at efficient osteogenic differentiation in the context of bone tissue engineering and regenerative medicine.

Acknowledgements

D.M. Jiang was supported by the National Natural Science Foundation of China (NSFC, 81472057) and the Natural Science Foundation Project of CQ CSTC (2009BB5410).

References

[1] A. K. Gaharwar, S. M. Mihaila, A. Swami, A. Patel, S. Sant, R. L. Reis, A. P. Marques, M. E. Gomes and A. Khademhosseini, Adv Mater **25**, 3329 (2013).
[2] J. Kim, H. N. Kim, K. T. Lim, Y. Kim, S. Pandey, P. Garg, Y. H. Choung, P. H. Choung, K. Y. Suh, J. H. Chung, Biomaterials **34**, 7257 (2013).
[3] W. G. De Long, Jr., T. A. Einhorn, K. Koval, M. McKee, W. Smith, R. Sanders, T. Watson, J bone joint surg Am **89**, 649 (2007).
[4] C. M. Rice, E. A. Mallam, A. L. Whone, P. Walsh, D. J. Brooks, N. Kane, S. R. Butler, D. I. Marks, N. J. Scolding, Clin pharmacol ther **87**, 679 (2010).
[5] S. S. Lee, B. J. Huang, S. R. Kaltz, S. Sur, C. J. Newcomb, S. R. Stock, R. N. Shah, S. I. Stupp, Biomaterials **34**, 452 (2013).
[6] P. V. Giannoudis, H. Dinopoulos and E. Tsiridis, Injury, **36 Suppl 3**, S20 (2005).
[7] S. Bose, M. Roy and A. Bandyopadhyay, Trends biotechnol **30**, 546 (2012).
[8] V. Mourino, A. R. Boccaccini, J R Soc Interface **7**, 209 (2010).
[9] B. He, X. Yuan, A. Zhou, H. Zhang, D. Jiang, Expert Rev Mol Med **16**, e12 (2014).
[10] J. Kisiday, M. Jin, B. Kurz, H. Hung, C. Semino, S. Zhang and A. J. Grodzinsky, Proc Natl Acad Sci USA **99**, 9996 (2002).
[11] H. Hosseinkhani, M. Hosseinkhani, F. Tian, H. Kobayashi and Y. Tabata, Tissue Eng **13**, 11 (2007).
[12] B. He, X. Yuan, J. Wu, Y. Bai, D. Jiang, Sci. Adv. Mater. **7**, 1221 (2015).
[13] S. H. Kim, W. Hur, J. E. Kim, H. J. Min, S. Kim, H. S. Min, B. K. Kim, S. H. Kim, T. H. Choi, Y. Jung, Tissue Eng Part A **21**, 1237 (2015).
[14] A. Li, A. Hokugo, A. Yalom, E. J. Berns, N. Stephanopoulos, M. T. McClendon, L. A. Segovia, I. Spigelman, S. I. Stupp, R. Jarrahy, Biomaterials, **35**, 8780 (2014).
[15] B. He, X. Yuan and D. Jiang, RSC Advances **4**, 23610 (2014).
[16] X. Yuan, B. He, Z. Lv and S. Luo, RSC Advances **4**, 53801 (2014).
[17] V. F. Segers and R. T. Lee, Circ Res, **109**, 910-922(2011).
[18] Y. Loo, Y. C. Wong, E. Z. Cai, C. H. Ang, A. Raju, A. Lakshmanan, A. G. Koh, H. J. Zhou, T. C. Lim, S. M. Moochhala, C. A. Hauser, Biomaterials **35**, 4805 (2014).
[19] A. Schneider, J. A. Garlick and C. Egles, PloS one **3**, e1410 (2008).
[20] A. Zhou, S. Chen, B. He, W. Zhao, X. Chen and D. Jiang, Drug des dev ther **10,** 3043 (2016) **.**
[21] S. Woerly, E. Pinet, L. de Robertis, D. Van Diep and M. Bousmina, Biomaterials, 2001, **22**, 1095 (2001).
[22] J. Graf, R. C. Ogle, F. A. Robey, M. Sasaki, G. R. Martin, Y. Yamada, H. K. Kleinman, Biochemistry **26**, 6896 (1987).
[23] M. Jucker, H. K. Kleinman, D. K. Ingram, J Neurosci Res **28**, 507 (1991).
[24] E. Ruoslahti, M. D. Pierschbacher, Cell **44**, 517 (1986).
[25] L. A. Smith Callahan, E. P. Childers, S. L. Bernard, S. D. Weiner, M. L. Becker, Acta Biomater **9**, 7420 (2013).
[26] Z. X. Zhang, Q. X. Zheng, Y. C. Wu, D. J. Hao, Biotechnol Bioeng **15**, 545 (2010).
[27] H. Duale, S. Hou, A. V. Derbenev, B. N. Smith, A. G. Rabchevsky, J Neuropathol Exp Neurol, **68**, 168 (2009).
[28] A. Subramanian, U. M. Krishnan, S. Sethuraman, J Biomed Sci **16**, 108(2009).
[29] M. C. Dodla and R. V. Bellamkonda, Biomaterials, **29**, 33 (2008).

[30] G. T. Christopherson, H. Song, H. Q. Mao, Biomaterials **30**, 556 (2009).
[31] S. Zhang, Nat Biotechnol **21**, 1171(2003).
[32] Z. Luo and S. Zhang, Chem Soc Rev **41**, 4736 (2012).
[33] Z. Luo, S. Wang and S. Zhang, Biomaterials **32**, 2013 (2011).
[34] J. Liu and X. Zhao, Nanomedicine (Lond) **6**, 1621 (2011).
[35] C. A. Hauser and S. Zhang, Chem Soc Rev **39**, 2780 (2010).
[36] Y. Yanlian, K. Ulung, W. Xiumei, A. Horii, H. Yokoi and Z. Shuguang, Nano Today **4**, 193 (2009).
[37] X. Zhao and S. Zhang, Chem Soc Rev, **35**, 1105-1110(2006).
[38] Y. Hong, R. L. Legge, S. Zhang and P. Chen, Biomacromolecules **4**, 1433 (2003).
[39] H. Hosseinkhani, H. Kobayashi and Y. Tabata, Peptide science, 22 (2006).
[40] H. Hosseinkhani, H. Kobayashi and Y. Tabata, Peptide science, 07 (2006).
[41] H. Hosseinkhani, M. Hosseinkhani and A. Khademhosseini, Yakhte Med. J **8**, 204 (2006).
[42] M. P. Lutolf and J. A. Hubbell, Nat Biotechnol **23**, 47 (2005).
[43] H. Hosseinkhani, M. Hosseinkhani, A. Khademhosseini, H. Kobayashi, Y. Tabata, Biomaterials, **27**, 5836 (2006).
[44] F. Gelain, L. D. Unsworth and S. Zhang, J Control Release **145**, 231 (2010).
[45] S. Koutsopoulos, L. D. Unsworth, Y. Nagai and S. Zhang, Proc Natl Acad Sci U S A, **106**, 4623 (2009).
[46] H. Hosseinkhani, M. Hosseinkhani, A. Khademhosseini, H. Kobayashi, J Control Release, **117**, 380 (2007).
[47] N. Stephanopoulos, J. H. Ortony, S. I. Stupp, Acta Mater **61**, 912 (2013).
[48] S. Aota, M. Nomizu and K. M. Yamada, J biol chem **269**, 24756 (1994).
[49] A. Horii, X. Wang, F. Gelain and S. Zhang, PloS one **2**, e190 (2007).
[50] J. M. Anderson, M. Kushwaha, A. Tambralli, S. L. Bellis, R. P. Camata, H. W. Jun, Biomacromolecules, **10**, 2935-2944(2009).
[51] J. Y. Lee, J. E. Choo, Y. S. Choi, J. S. Suh, S. J. Lee, C. P. Chung, Y. J. Park, Biomaterials **30**, 3532 (2009).
[52] X. Jiang, H. Q. Cao, L. Y. Shi, S. Y. Ng, L. W. Stanton and S. Y. Chew, Acta Biomater, **8**, 1290 (2012).
[53] G. Kaur, C. Wang, J. Sun and Q. Wang, Biomaterials **31**, 5813 (2010).
[54] T. D. Sargeant, M. O. Guler, S. M. Oppenheimer, A. Mata, R. L. Satcher, D. C. Dunand, S. I. Stupp, Biomaterials **29**, 161 (2008).
[55] J. C. Igwe, P. E. Mikael, S. P. Nukavarapu, J Tissue Eng Regen Med **8**, 131 (2014).